Eur. Phys. J. Plus (2015) **130**: 111
DOI 10.1140/epjp/i2015-15111-8

THE EUROPEAN PHYSICAL JOURNAL PLUS

Regular Article

Modulational instability of polarized beams in nonlocal media with stochastic parameters

H. Tagwo[1,a], A. Mohamadou[2,3,b], Alim[4,c], C.G. Latchio Tiofack[1,d], and T.C. Kofane[1,e]

[1] Department of Physics, Faculty of Science, University of Yaounde I, P.O. Box 812, Yaounde, Cameroon
[2] Department of Physics, Faculty of Science, University of Maroua, P.O. Box 814, Maroua, Cameroon
[3] The Abdus Salam International Centre for Theoretical Physics, P.O. Box 538, Strada costiera 11, I-34014, Trieste, Italy
[4] Department of Science Physics, Higher Teacher Training College, University of Maroua, P.O. Box 55, Maroua, Cameroon

Received: 1 January 2015 / Revised: 15 March 2015
Published online: 12 June 2015 –

Abstract. We investigate analytically and numerically the modulational instability (MI) in a nonlinear optical fiber. We use a generalized model describing the pulse propagation of waveguiding structure composed of two adjacent waveguides, where the effect of nonlocal nonlinear response as well as stochastic coefficients are taken into account. Applying the linear stability analysis and stochastic calculus, we show that the MI gain spectra reads as the maximal eigenvalue of a constant matrix. The generic properties of the MI gain spectra are then demonstrated for the rectangular response function. We observe that random inhomogeneities extend the domain of the homogeneous MI gain spectra over the whole spectrum of modulation, and the nonlocality parameter reduces drastically the growth rate and bandwidth of instability caused by stochasticity both in anomalous and normal dispersion regimes. We observe also that MI does not appears for all values of the nonlocal parameter. Numerical simulations of the full stochastic system of nonlinear Schrödinger equations describing the dynamics of the waves are carried out and lead to the generation of a train of pulses.

1 Introduction

In the last two decades or so, there has been a considerable interest in wave propagation phenomena that involve intensity-dependent processes in a host of optical systems. In particular, propagation of intense continuous waves in dielectric media leads to several major nonlinear phenomena having fundamental interests and practical applications. A well-known example of those phenomena is the modulational instability (MI), which arises out of the interplay between the dispersive and nonlinear effects, and which manifests itself in the exponential growth of weak perturbations [1,2]. The gain leads to amplification of sidebands, which break up the otherwise uniform wave and generate fine localized structures. Thus, it may act as a precursor for the formation of solitons. The phenomenon of MI has been identified and studied in various physical systems, such as fluids [3], plasma [4], nonlinear optics [5], discrete nonlinear systems [6], and in quadratic nonlinear lattices [7] to cite a few. It has been shown that MI is strongly affected by mechanisms such as saturation of nonlinearity [8], coherence properties of optical beams [9], linear and nonlinear gratings [10], nonlocality of the nonlinearity [11], competing local and nonlocal nonlinearity [12], nonlocal $\chi(2)$- model [13] and generation of super-continuum spectra [14,15], and so on. Recently, people in fiber-optic sensing have embraced MI as a novel sensing mechanism, in which the shift in the gain band is tracked *versus* the change in a given quantity that one wants to measure. It has been shown that MI allows highly sensitive biosensing [16], refractive index sensing [17], and even strain sensing [18]. The MI gain in homogeneous medium has been extensively studied for the scalar nonlinear Schrödinger equation (NLSE) [19], and also for the vector NLSE both in normal [20] and anomalous [21] regimes. It has been shown that MI depends on the frequency and power of initial modulation . However, in realistic fiber transmission

[a] e-mail: hippocritique@yahoo.fr
[b] e-mail: mohdoufr@yahoo.fr
[c] e-mail: alimdia@yahoo.fr
[d] e-mail: glatchio@yahoo.fr
[e] e-mail: tckofane@yahoo.com

links, the chromatic dispersion and nonlinearity are not constant, but can fluctuate stochastically around their mean values. The inhomogeneity of the medium may be inherent to the medium [22] or induced by other propagating waves [23]. Recently, it was pointed out that the random inhomogeneities in nonlinear dispersive media may extend the domain of the homogeneous MI of nonlinear plane waves over the whole spectrum of modulations, even for the normal dispersion regime. Indeed, previous works have analyzed the MI of electromagnetic waves in nonlinear Kerr media with random nonlinearity [24] or random group-velocity dispersion [25]. Spatial nonlocality, which is already an established concept in plasma physics [26,27], means that the response of the medium at a particular point is not determined solely by the wave intensity at that point (as in local media), but also depends on the wave intensity in its vicinity. The nonlocal nature often results from a transport process, such as atom diffusion [28], heat transfer [29, 30], or drift of electric charges [31]. In the study of MI, it was shown in [32] that nonlocality changes drastically the growth rate and bandwidth of instability caused by stochasticity of parameters of a Kerr medium. But this study was limited to the case of scalar waves. It was demonstrated recently that vector soliton structures exhibit properties that have no counterpart in the scalar case [33].

Polarized vector solitons, first proposed by Manakov [34], consist of two orthogonally polarized components in a nonlinear Kerr media in which self-phase modulation is identical to cross-phase modulation. The nonlinear action of a field component on itself equals the action of one component on the other [34]. The Manakov model can support different classes of vector soliton pairs, namely, bright-bright [35], dark-dark [36], and bright-dark [36] solitons pairs. The polarized vector dark-dark solitons have been investigated in local media using the inverse scattering transform method [36] and the Hirota method [35,37]. However, recent research has shown that nonlocality promotes the stability of vector solitons and plays an important role in the formation of vector dipole solitons [38], multipole solitons [39], two-color solitons [40], vortex solitons [41], and necklace solitons [42]. Thus the generation of solitonlike excitations in nonlocal media is an important and significant subject.

In this work, we focus on the generation of solitonlike excitations in a nonlocal Kerr-type media with stochastic parameters through the MI. With this aim, using the stochastic calculus and linear stability analysis we derive a MI gain matrix in which the positive eigenvalue leads to instabilities. The work is organized as follows: In sect. 2, we presented a model of coupled system in optical fiber. In sect. 3, we study the linear stability analysis of this model equation. The second-order moments MI is analyzed in sect. 4. Then in sect. 5, we perform a direct numerical integration of the coupled one-dimensional nonlinear Schrödinger equation to verify the MI numerically for nonlocality parameter. Section 6 is devoted to the conclusion.

2 The model

The propagation of two orthogonally polarized beams in nonlocal media with random parameters is described by the two scalar NLS equations given by [43]:

$$
\begin{aligned}
&i\frac{\partial u_+}{\partial z}+\frac{1}{2}\beta_1(z)\frac{\partial^2 u_+}{\partial x^2}-\gamma_1(z)u_+\int_{-\infty}^{+\infty}R\left(x-x^{'}\right)\left[\left|u_+\left(x^{'},z\right)\right|^2+g_{12}\left|u_-\left(x^{'},z\right)\right|^2\right]\mathrm{d}x^{'}=0,\\
&i\frac{\partial u_-}{\partial z}+\frac{1}{2}\beta_2(z)\frac{\partial^2 u_-}{\partial x^2}-\gamma_2(z)u_-\int_{-\infty}^{+\infty}R\left(x-x^{'}\right)\left[g_{12}\left|u_+\left(x^{'},z\right)\right|^2+\left|u_-(x^{'},z)\right|^2\right]\mathrm{d}x^{'}=0,
\end{aligned}
\tag{1}
$$

where, $u_+=u_+(x,z)$ and $u_-=u_-(x,z)$ are the complex envelope amplitudes of two arbitrary but orthogonal polarizations. x and z are, respectively, the transverse and propagation coordinates. g_{12} represent the coupling coefficient of the two polarizations mode fiber. The dispersion coefficients $\beta_j(z)$, and nonlinearity coefficients $\gamma_j(z)$, $(j=1,2)$ are considered as stochastic functions which fluctuate around their mean values β_{0j} and γ_{0j}:

$$
\begin{aligned}
\beta_j(z)&=\beta_{j0}(1+m_{\beta_j}(z)),\\
\gamma_j(z)&=\gamma_{j0}(1+m_{\gamma_j}(z)),
\end{aligned}
\tag{2}
$$

$m_{\beta_j}(z)$ and $m_{\gamma_j}(z)$ are independent zero-mean random processes of the Gaussian white-noise type,

$$
\begin{aligned}
\langle m_{\beta_j}(z)\rangle&=\langle m_{\gamma_j}(z)\rangle=0,\\
\langle m_{\beta_i}(z)m_{\beta_j}(z^{'})\rangle&=2\sigma^2_{\beta_j}\delta_{ij}\delta(z-z^{'}),\\
\langle m_{\gamma_i}(z)m_{\gamma_j}(z^{'})\rangle&=2\sigma^2_{\gamma_j}\delta_{ij}\delta(z-z^{'}),\\
\langle m_{\gamma_i}(z)m_{\beta_j}(z^{'})\rangle&=0.
\end{aligned}
\tag{3}
$$

The angular brackets stand for the expectation with respect to the distribution of the processes $m_{\beta_j}(z)$ and $m_{\gamma_j}(z)$. $m_{\beta_j}(z)$ and $m_{\gamma_i}(z)$ are uncorrelated. The form of the convolution integral represents the nonlocal nonlinear

response. The actual form of the nonlocal response is determined by the details of the physical process responsible for the nonlocality. For all diffusion-type nonlinearities [44], for orientational-type nonlinearities (like nematic liquid crystal) [45], and for the general quadratic nonlinearity describing parametric interaction [46–48], the response function is an exponential $R(x) = (2a)^{-1}\exp(-|x|/a)$ originating from a Lorentzian in the Fourier domain, with a defining the degree of nonlocality. Many classes of response functions actually have generic properties in terms of MI, as done in [49].

For the sake of simplicity and analytical tractability and without loss of generality, however, we consider here the rectangular profile for the nonlocal response function $R(x)$ [32]:

$$R(x) = \begin{cases} \frac{1}{2a}, & -a \le x \le a, \\ 0, & \text{otherwise}, \end{cases} \tag{4}$$

where normalization condition $\int_{-\infty}^{+\infty} R(x)\mathrm{d}x = 1$, is satisfied. In particular, when $a = 0$, we can get $R(x) = \delta(x)$, which correspond a standard local Kerr media. When a tends to $+\infty$, eq. (1) becomes linear and the solitons are known as accessible solitons [50]. Although eq. (4) is only a phenomenological model, it also can describe the general properties of the nonlocal media very well [51].

3 The linear stability analysis

The fundamental framework of MI analysis relies on the linear stability analysis, such that a continuous wave (CW) solution is perturbed by a small amplitude or phase perturbation satisfying the condition $|a_j(z,x)|^2 \ll |P_0|^2$, and then study whether the perturbation amplitude grows or decays with propagation. The symmetric or antisymmetric CW steady-state solution can be written as

$$\begin{aligned} u_+(z,x) &= P_0 \exp i\left(P_0^2 + g_{12}P_1^2\right)\int_0^z \gamma_1(z')\mathrm{d}z', \\ u_-(z,x) &= P_1 \exp i\left(P_1^2 + g_{12}P_0^2\right)\int_0^z \gamma_2(z')\mathrm{d}z', \end{aligned} \tag{5}$$

where, P_0 and P_1 are the power of plane wave solution of eq. (1). The stability of the steady state can be examined by introducing a perturbed field by assuming that

$$\begin{aligned} u_+(z,x) &= [P_0 + u(z,x)] \exp i\left(P_0^2 + g_{12}P_1^2\right)\int_0^z \gamma_1(z')\mathrm{d}z', \\ u_-(z,x) &= [P_1 + v(z,x)] \exp i\left(P_1^2 + g_{12}P_0^2\right)\int_0^z \gamma_2(z')\mathrm{d}z', \end{aligned} \tag{6}$$

$u(z,x)$ and $v(z,x)$ being a small complex modulation. Substituting eq. (6) into eq. (1) and linearizing about the plane wave (5), we get a linear equation for $u(z,x)$ and $v(z,x)$:

$$\begin{aligned} i\frac{\partial u}{\partial z} + \frac{1}{2}\beta_1(z)\frac{\partial^2 u}{\partial x^2} - 2\gamma_1(z)\int_{-\infty}^{+\infty} R(x-x')(P_0^2 Re(u) + g_{12}P_0P_1 Re(v))\mathrm{d}x' = 0, \\ i\frac{\partial v}{\partial z} + \frac{1}{2}\beta_1(z)\frac{\partial^2 v}{\partial x^2} - 2\gamma_2(z)\int_{-\infty}^{+\infty} R(x-x')(P_1^2 Re(v) + g_{12}P_0P_1 Re(u))\mathrm{d}x' = 0. \end{aligned} \tag{7}$$

Performing the Fourier-transform, $\hat{u} = \int u\exp(-ikx)\mathrm{d}x$, $\hat{v} = \int v\exp(-ikx)\mathrm{d}x$ and using the complex representation, $\hat{u} = \hat{u}_r + i\hat{u}_i$, $\hat{v} = \hat{v}_r + i\hat{v}_i$, eq. (7) is converted to a system of linear equations:

$$\frac{\mathrm{d}}{\mathrm{d}z}\begin{pmatrix} \hat{u}_r \\ \hat{v}_r \\ \hat{u}_i \\ \hat{v}_i \end{pmatrix} = \begin{pmatrix} 0 & 0 & \frac{1}{2}\beta_1 k^2 & 0 \\ 0 & 0 & 0 & \frac{1}{2}\beta_2 k^2 \\ -\frac{1}{2}\beta_1 k^2 - 2\gamma_1 P_0^2\hat{R} & -2\gamma_1 g_{12}P_0P_1\hat{R} & 0 & 0 \\ -2\gamma_2 g_{12}P_0P_1\hat{R} & -\frac{1}{2}\beta_2 k^2 - 2\gamma_2 P_1^2\hat{R} & 0 & 0 \end{pmatrix}\begin{pmatrix} \hat{u}_r \\ \hat{v}_r \\ \hat{u}_i \\ \hat{v}_i \end{pmatrix}. \tag{8}$$

If we were dealing with a deterministic system with paramater, β_{10}, β_{20}, γ_{10}, γ_{20}, eq. (8) would be the main object used to study MI. However, MI induced by random fluctuations is not captured by the analysis of the first moments, $\langle\hat{u}_r\rangle$, $\langle\hat{v}_r\rangle$, $\langle\hat{u}_i\rangle$, $\langle\hat{v}_i\rangle$ [52–54]. It is therefore necessary to compute the modulational intensity growth given by the higher-order moments.

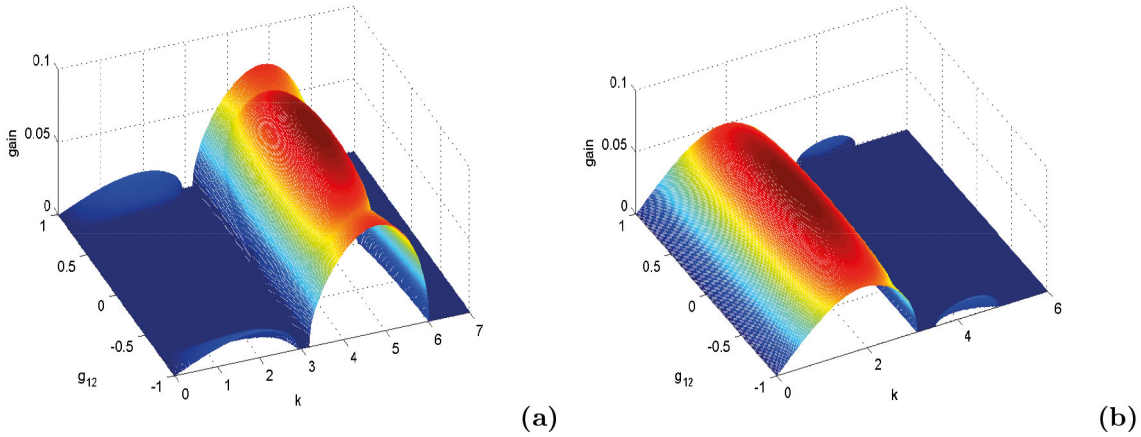

Fig. 1. The MI gain $G_2(k)$ in local media with nonstochastic parameters. (a) for anomalous dispersion regimes ($\beta_{01} = -2.5\,\mathrm{ps}^2/\mathrm{km}$, $\beta_{02} = -2.5\,\mathrm{ps}^2/\mathrm{km}$), (b) normal dispersion regime ($\beta_{01} = 2.5\,\mathrm{ps}^2/\mathrm{km}$, $\beta_{02} = 2.5\,\mathrm{ps}^2/\mathrm{km}$). Other parameters are $a = 1$, $\sigma^2_{\beta_j} = \sigma^2_{\gamma_j} = 0.0$, $j = 1, 2$, $P_0 = P_1 = 10\,\mathrm{W}$, $\gamma_{01} = \gamma_{02} = 3\,\mathrm{W}^{-1}/\mathrm{km}$.

4 The second-order moment MI gain

We consider the second moments, $\langle\hat{u}_r^2\rangle$, $\langle\hat{v}_r^2\rangle$, $\langle\hat{u}_i^2\rangle$, $\langle\hat{v}_i^2\rangle$, $\langle\hat{u}_r\hat{v}_r\rangle$, $\langle\hat{u}_i\hat{v}_i\rangle$, $\langle\hat{u}_r\hat{u}_i\rangle$, $\langle\hat{v}_r\hat{v}_i\rangle$, $\langle\hat{u}_r\hat{v}_i\rangle$, $\langle\hat{v}_r\hat{u}_i\rangle$, for the vector $X^{(2)}$. The moments, $\langle\hat{u}_r\hat{v}_r\rangle$, $\langle\hat{u}_i\hat{v}_i\rangle$, $\langle\hat{u}_r\hat{u}_i\rangle$, $\langle\hat{v}_r\hat{v}_i\rangle$, $\langle\hat{u}_r\hat{v}_i\rangle$, $\langle\hat{v}_r\hat{u}_i\rangle$, are added to close equations for the second-order moments. Then, we should evaluate the spaces evolution of the vector $X^{(2)}$. Its first component gives

$$\frac{\mathrm{d}}{\mathrm{d}z}\langle\hat{u}_r^2\rangle = \frac{1}{2}k^2\beta_{10}\langle\hat{u}_r\hat{u}_i\rangle + \frac{1}{2}k^2\beta_{10}\langle\hat{u}_r\hat{u}_i m_{\beta_{10}}(z)\rangle. \tag{9}$$

For decoupling of the means, $\langle\hat{u}_r\hat{u}_i m_{\beta_{10}}(z)\rangle$, we apply the Furutzu-Novikov formulas [55,56]

$$\begin{aligned}\langle m_{\beta_{j0}}(z)F\rangle &= \sigma^2_{\beta_j}\int B(z-z')\left\langle\frac{\delta}{\delta m_{\beta_{j0}}}F\right\rangle\mathrm{d}z',\\ \langle m_{\gamma_{j0}}(z)F\rangle &= \sigma^2_{\gamma_j}\int B(z-z')\left\langle\frac{\delta}{\delta m_{\gamma_{j0}}}F\right\rangle\mathrm{d}z', \quad j=1,2.\end{aligned} \tag{10}$$

Here, $B(z-z') = \delta(z-z')$ for a white-noise Gaussian random process. Finally, we obtain the equation of the first component

$$\frac{\mathrm{d}}{\mathrm{d}z}\langle\hat{u}_r^2\rangle = \frac{1}{2}k^2\beta_{10}\langle\hat{u}_r\hat{u}_i\rangle + \frac{1}{2}k^4\sigma^2_{\beta_1}\beta^2_{10}\left(\langle\hat{u}_i^2\rangle - \langle\hat{u}_r^2\rangle\right). \tag{11}$$

In the same way we can evaluate the derivation of the other components of the vector $X^{(2)}$. As a result, we obtain the system for the second moments which read as a linear system

$$\frac{\mathrm{d}}{\mathrm{d}z}X^{(2)} = M^{(2)}X^{(2)}, \tag{12}$$

where, $X^{(2)}$ and $M^{(2)}$ are defined in appendix. The matrix $M^{(2)}$ has ten eigenvalues which can be positive or negative. Eigenvalues of $M^{(2)}$ with positive real parts lead to instabilities, and the largest positive value determines the MI gain $G_2(k)$. In the below discussion we will assume that the fluctuations of stochastic parameters are weak, *i.e* $\sigma^2_{\beta_j} \ll |\beta_{j0}|, \sigma^2_{\gamma_j} \ll |\gamma_{j0}|$, $j = 1, 2$. We recall that in deterministic medium where the nonlinear response is local, the plotting of MI gain relatively to the wave number k for the situation of anomalous dispersion regime *i.e* $\beta_{0j} < 0$, $(j = 1, 2)$ shows in fig. 1(a) one conventional sideband. In the case of normal dispersion regime *i.e* $\beta_{0j} > 0$, fig. 1(b) also shows one conventional band. Figure 2(a) shows for anomalous dispersion case the gain spectra in nonlocal media with nonstochastic parameters; we can see many non-conventional sidebands which appear for certain values of nonlocal parameters. The normal dispersion case is shown in fig. 2(b) where we can also observe many non-conventional sideband. The maximum MI gain is obtained for the higher values of the wave number k. The higher value of the MI gain decreases with the increasing value of a, thus nonlocality clearly tends to suppress MI. The number of non-conventional bands increases for the mixture regime (anomalous and normal dispersion regimes) as depicted in fig. 2(c). While the width of the sideband becomes narrow, the maximum on MI gain induced by nonlocal effect fluctuates.

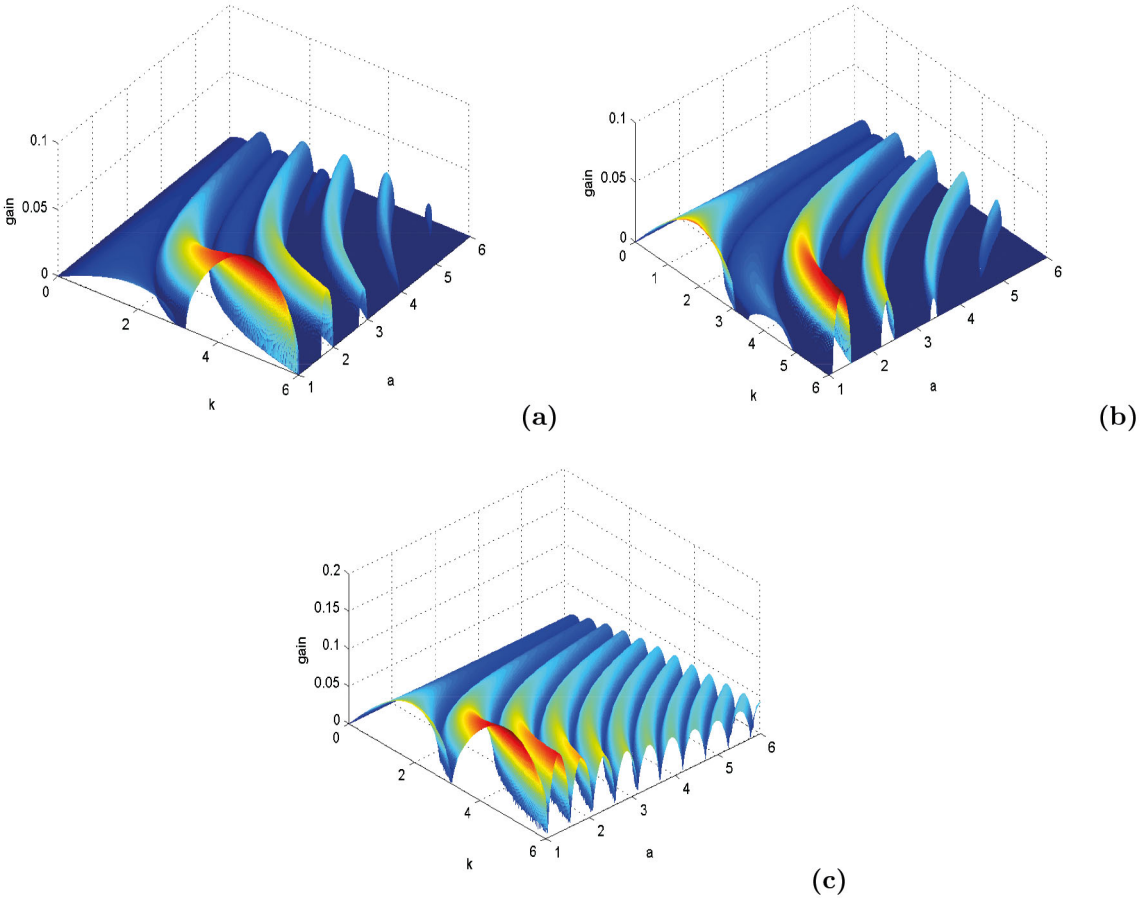

Fig. 2. The MI gain $G_2(k)$ in nonlocal media with nonstochastic parameters. (a) for anomalous dispersion regime ($\beta_{01} = -2.5\,\mathrm{ps}^2/\mathrm{km}$, $\beta_{02} = -2.5\,\mathrm{ps}^2/\mathrm{km}$), (b) normal dispersion regime ($\beta_{01} = 2.5\,\mathrm{ps}^2/\mathrm{km}$, $\beta_{02} = 2.5\,\mathrm{ps}^2/\mathrm{km}$), (c) mixed regime ($\beta_{01} = 2.5\,\mathrm{ps}^2/\mathrm{km}$, $\beta_{02} = -2.5\,\mathrm{ps}^2/\mathrm{km}$). Other parameters are $g_{12} = 1$, $\sigma^2_{\beta_j} = \sigma^2_{\gamma_j} = 0.0$, $j = 1, 2$, $P_0 = P_1 = 10\,\mathrm{W}$, $\gamma_{01} = \gamma_{02} = 3\,\mathrm{W}^{-1}/\mathrm{km}$.

Let us now take into account the both effects (stochasticity and the nonlocal response). Figures 3(a) and 3(b) are plotted for the anomalous regime. Figures 3(c), 3(d) show, respectively, the MI gain spectrum for normal and mixed dispersion regimes. One can see that the number of non-conventional sidebands increase for the case of the mixed regime. We observe also that the amplitude of sidebands is raised for the lower wave numbers and decrease gradually for the higher wave numbers. The number of side lobes increase in the mixture regime, while the width of the sideband decreases. We also plot the gain relatively to σ_β and we note that the modulation amplitude of the non-conventional band increases with the growth of k.

5 Numerical simulations in different GVD domains

In this section we perform direct numerical integrations of the CNLSE (1) by using the split-step Fourier [19]. The numerical simulations have been carried out using various step sizes down to 0.0001 throughout the z-direction with up to 1024 points along the x-direction. Then, system of eq. (1) is splitted into its linear part,

$$\frac{\partial u_+}{\partial z} = \frac{1}{2} i\beta_{10}[1 + m_{\beta_1}(z)]\frac{\partial^2 u_+}{\partial x^2}\,,$$
$$\frac{\partial u_-}{\partial z} = \frac{1}{2} i\beta_{20}[1 + m_{\beta_2}(z)]\frac{\partial^2 u_-}{\partial x^2}\,, \tag{13}$$

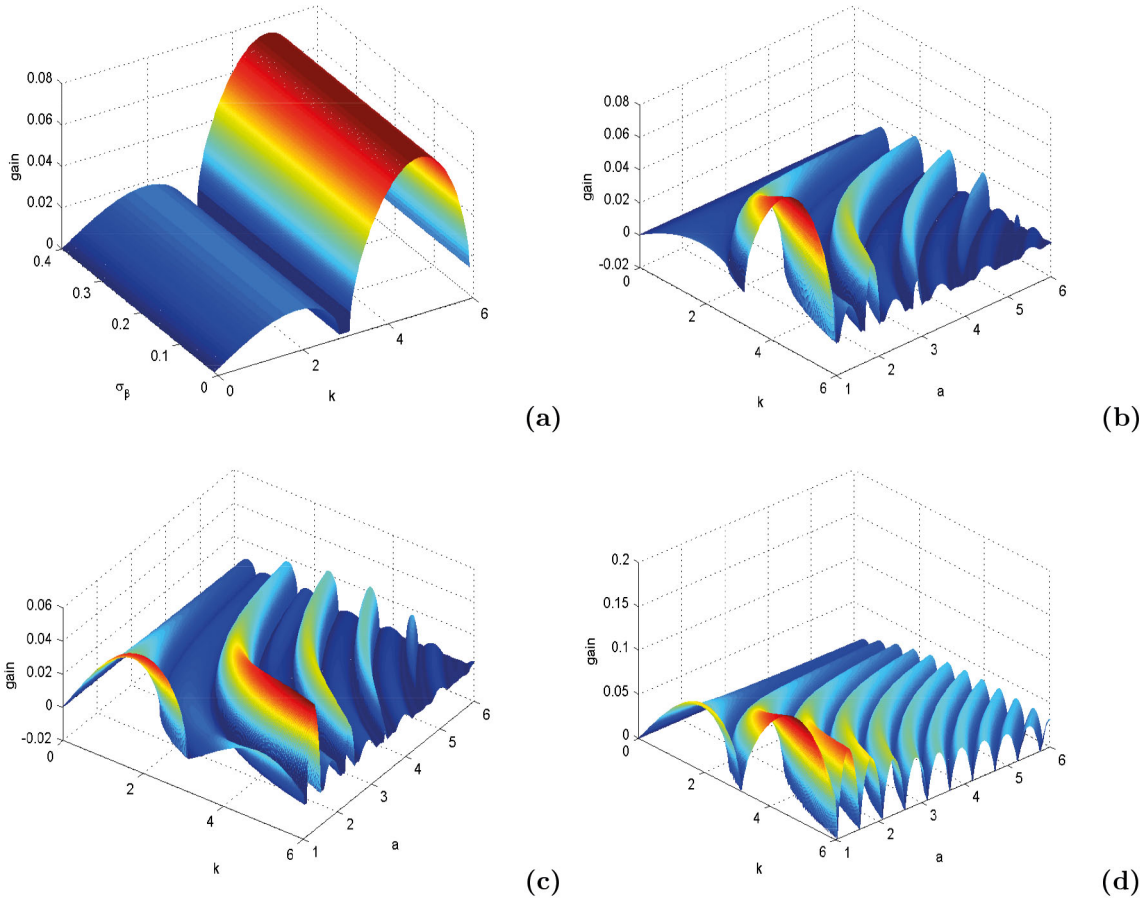

Fig. 3. The MI gain $G_2(k)$ in nonlocal media with stochastic parameters. (a), (b) for anomalous dispersion regime ($\beta_{01} = -2.5\,\mathrm{ps}^2/\mathrm{km}$, $\beta_{02} = -2.5\,\mathrm{ps}^2/\mathrm{km}$), (c) normal dispersion regime ($\beta_{01} = 2.5\,\mathrm{ps}^2/\mathrm{km}$, $\beta_{02} = 2.5\,\mathrm{ps}^2/\mathrm{km}$), (d) mixed regime ($\beta_{01} = 2.5\,\mathrm{ps}^2/\mathrm{km}$, $\beta_{02} = -2.5\,\mathrm{ps}^2/\mathrm{km}$). Other parameters are $g_{12} = 1$, $\sigma^2_{\beta_j} = \sigma^2_{\gamma_j} = 1.6$, $j = 1, 2$, $P_0 = P_1 = 10\,\mathrm{W}$, $\gamma_{01} = \gamma_{02} = 3\,\mathrm{W}^{-1}/\mathrm{km}$.

and its nonlinear part,

$$\frac{\partial u_+}{\partial z} = -i\gamma_{10}[1 + m_{\gamma_1}(z)]u_+ \int_{-\infty}^{+\infty} R\left(x - x'\right)\left[\left|u_+\left(x', z\right)\right|^2 + g_{12}\left|u_-\left(x', z\right)\right|^2\right] \mathrm{d}x',$$
$$\frac{\partial u_-}{\partial z} = -i\gamma_{20}[1 + m_{\gamma_2}(z)]u_- \int_{-\infty}^{+\infty} R\left(x - x'\right)\left[\left|u_-\left(x', z\right)\right|^2 + g_{12}\left|u_+\left(x', z\right)\right|^2\right] \mathrm{d}x'. \quad (14)$$

The solution of the linear part is approximated by

$$u_+(x, z + \mathrm{d}z) = F^{-1}\left\{F[u_+(x, z)] \exp\left[-0.5\beta_{10}\left(1 + \frac{m_{\beta_1(z)}}{\sqrt{\mathrm{d}z}}\right)k^2 \mathrm{d}z\right]\right\},$$
$$u_-(x, z + \mathrm{d}z) = F^{-1}\left\{F[u_-(x, z)] \exp\left[-0.5\beta_{20}\left(1 + \frac{m_{\beta_2(z)}}{\sqrt{\mathrm{d}z}}\right)k^2 \mathrm{d}z\right]\right\}, \quad (15)$$

where F denotes the Fourier-transform and F^{-1} its inverse. The solution of the nonlinear part can be approximated by

$$u_+(x, z + \mathrm{d}z) = u_+(x, z)F^{-1}\exp[N_1(z)\mathrm{d}z],$$
$$u_-(x, z + \mathrm{d}z) = u_-(x, z)F^{-1}\exp[N_2(z)\mathrm{d}z], \quad (16)$$

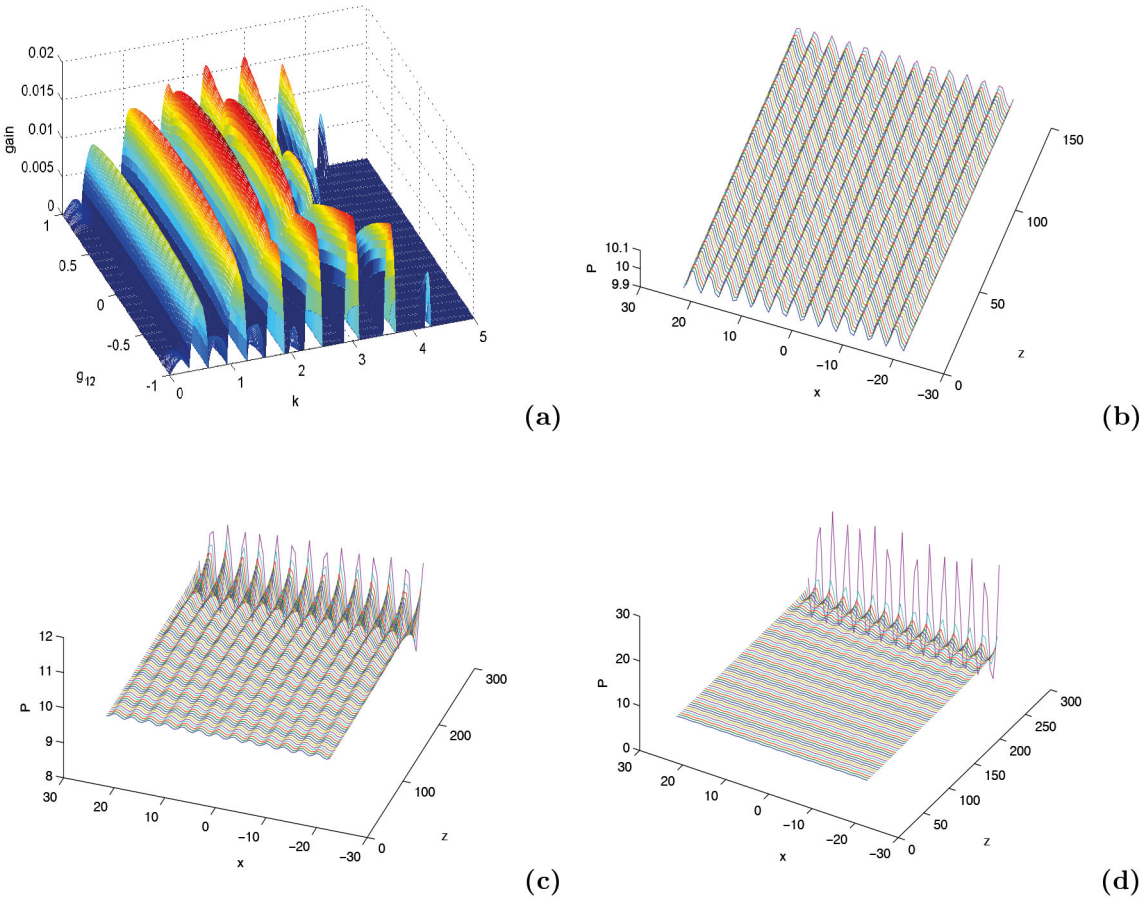

Fig. 4. (a) The MI gain $G_2(k)$ in local media with nonstochastic parameters for the anomalous dispersion regimes. Propagation of the wave in the anomalous dispersion regime showing effects of the fluctuation parameters. Parameters of the system are $\beta_{01} = \beta_{02} = -2.5\,\mathrm{ps}^2/\mathrm{km}$, $\gamma_{01} = \gamma_{02} = 3\,\mathrm{W}^{-1}/\mathrm{km}$, $a = 10$, $P_0 = P_1 = 10\,\mathrm{W}$. (b) For stable oscillations, $\sigma^2_{\beta_j} = \sigma^2_{\gamma_j} = 0.2$, $j = 1, 2$; and (c) and (d) for instability $\sigma^2_{\beta_j} = \sigma^2_{\gamma_j} = 0.28$.

where

$$N_1(z) = \gamma_{10}\left[\hat{R}(|\hat{u_+}|^2 + g_{12}|\hat{u_-}|^2)\left(1 + \frac{m_{\beta_1(z)}}{\sqrt{dz}}\right)\right],$$
$$N_2(z) = \gamma_{20}\left[\hat{R}(g_{12}|\hat{u_+}|^2 + |\hat{u_-}|^2)\left(1 + \frac{m_{\beta_2(z)}}{\sqrt{dz}}\right)\right], \tag{17}$$

where $\hat{u_+}$, $\hat{u_-}$ denotes the Fourier transform of u_+ and u_-. We use the Gaussian-distributed random numbers generated by a standard Box-Muller algorithm [57] as a model for the random process m_{β_j} and m_{γ_j}, $j = 1, 2$. The initial condition used is

$$u_+(0, x) = \sqrt{P_0}(1 + 0.003\cos(0.6\pi x)),$$
$$u_-(0, x) = \sqrt{P_1}(1 + 0.003\cos(0.6\pi x)). \tag{18}$$

The instability development depends on the value of nonlocality parameter and the fluctuation coefficients. Figure 4(a) presents the MI gain spectra. Results from numerical simulations of MI in the anomalous dispersion regime for different stochastic paramaters are presented in figs. 4(b), 4(c) and 4(d). For $\sigma^2_{\beta_j} = \sigma^2_{\gamma j} = 0.2$, we obtain that the propagation of waves remains stable as shown in fig. 4(b). Waves keep their shape and their amplitude remains constant during the propagation. The pulse can propagate stably in the given distance, even in the presence of the stochastic nonlinear terms. The evolution of the initial continuous wave up to a distance $z = 300\,\mathrm{m}$ is shown in figs. 4(c) and 4(d) for ($\sigma^2_{\beta_j} = \sigma^2_{\gamma_j} = 0.28$). It found that the pulse can propagate stably up to a distance of $z = 275\,\mathrm{m}$ in the anomalous dispersion regime. Over that distance, the quasi-continuous wave pulse disintegrates during propagation, leading to

filaments or break-up into pulse trains. This pulse train has the shape of a soliton-like object. MI typically occurs in the same parameter region where another universal phenomenon, soliton occurrence, is observed. Solitons are stationary localized wave packets (wave packets that never broaden) that share many features with real particles. Solitons can be intuitively understood as a result of the balance between the broadening tendency of diffraction (or dispersion) and nonlinear self-focusing.

In MI zones, the initial continuous wave tends to be disintegrated into a train of solitonlike objects. Attenuation waves are also observed during the propagation. However, when the modulational wave number is out of the MI zones, the trains of solitons disappear progressively and form a constant background solution. We have also found that increasing the stochastic parameters contributes to the MI phenomenon with pulse train which are generated. The present result, especially the formation of the stable periodic array of localized pulses, may find straightforward application in nonlinear optics.

6 Conclusion

We have investigated the MI of two orthogonally polarized incoherent beams in nonlocal media with stochastic parameters. Using the linear stability analysis and random process theory, we have obtained for the white-noise model of parameter fluctuations, the equations that govern the dependence of the MI gain on the modulation wave number. We have seen that the MI is not observed for all values of the nonlocal parameter (figs. 2(a), 2(b)). Contrary to the deterministic media where non-conventional sidebands appear due to fourth-order dispersion, several non-conventional sidebands appear here, for mixed regime (fig. 2(c)), or due to the presence of both effects of stochasticity and nonlocality (figs. 3(c), 3(d)). We have simulated the full system to determine the outcome of the development of the MI. It was found that depending on the fluctuation coefficients, the MI leads to a pattern in the form of a periodic pulse array. But in the random nonlinear case, the MI leads to the generation of a chain of chaotic pulses.

AM acknowleges financial support from the Abdus Salam International Center for Theoretical Physics (ICTP), Trieste, Italy through the Associate Programme. The work has greatly benefited from rich comments of the referees.

Appendix A.

The matrix elements of eq. (12) are given by

$$X^{(2)} = [\langle \hat{u}_r^2\rangle\langle \hat{v}_r^2\rangle\langle \hat{u}_i^2\rangle\langle \hat{v}_i^2\rangle\langle \hat{u}_r\hat{v}_r\rangle\langle \hat{u}_i\hat{v}_i\rangle\langle \hat{u}_r\hat{u}_i\rangle\langle \hat{v}_r\hat{v}_i\rangle\langle \hat{u}_r\hat{v}_i\rangle\langle \hat{v}_r\hat{u}_i\rangle]^T,$$

$$M^{(2)} = [M_1\, M_2\, M_3\, M_4\, M_5\, M_6\, M_7\, M_8\, M_9\, M_{10}],$$

with

$$M_1 = \begin{pmatrix} -\frac{1}{2}\sigma_{\beta_1}^2\beta_{10}^2k^4 \\ 0 \\ \frac{1}{2}\sigma_{\beta_1}^2\beta_{10}^2k^4 + 4\sigma_{\gamma_1}^2\gamma_{10}^2P_0^4\hat{R}^2 \\ 4\sigma_{\gamma_2}^2g_{12}^2\gamma_{20}^2P_0^2P_1^2\hat{R}^2 \\ 0 \\ 0 \\ -\frac{1}{2}\beta_{10}k^2 + 2\gamma_{10}P_0^2\hat{R} \\ 0 \\ 2g_{12}\gamma_{20}P_0P_1\hat{R} \\ 0 \end{pmatrix}, \quad M_2 = \begin{pmatrix} 0 \\ -\frac{1}{2}\sigma_{\beta_2}^2\beta_{20}^2k^4 \\ 4\sigma_{\gamma_1}^2g_{12}^2\gamma_{10}^2P_0^2P_1^2\hat{R}^2 \\ -\frac{1}{2}\sigma_{\beta_2}^2\beta_{20}^2k^4 + 4\sigma_{\gamma_2}^2\gamma_{20}^2P_1^4\hat{R}^2 \\ 0 \\ 0 \\ 0 \\ -\frac{1}{2}\beta_{20}k^2 + 2\gamma_{20}P_1^2\hat{R} \\ 0 \\ 2g_{12}\gamma_{10}P_0P_1\hat{R} \end{pmatrix},$$

$$M_3 = \begin{pmatrix} \frac{1}{2}\sigma_{\beta_1}^2\beta_{10}^2k^4 \\ 0 \\ -\frac{1}{2}\sigma_{\beta_1}^2\beta_{10}^2k^4 \\ 0 \\ 0 \\ 0 \\ \frac{1}{2}\beta_{10}k^2 \\ 0 \\ 0 \\ 0 \end{pmatrix}, \quad M_4 = \begin{pmatrix} 0 \\ \frac{1}{2}\sigma_{\beta_2}^2\beta_{20}^2k^4 \\ 0 \\ -\frac{1}{2}\sigma_{\beta_2}^2\beta_{20}^2k^4 \\ 0 \\ 0 \\ 0 \\ \frac{1}{2}\beta_{20}k^2 \\ 0 \\ 0 \end{pmatrix},$$

$$M_5 = \begin{pmatrix} 0 \\ 0 \\ 8\sigma_{\gamma_1}^2 g_{12}\gamma_{10}^2 P_0^3 P_1 \hat{R}^2 \\ 8\sigma_{\gamma_2}^2 g_{12}\gamma_{20}^2 P_0 P_1^3 \hat{R}^2 \\ -\frac{1}{2}\sigma_{\beta_1}^2\beta_{10}^2k^4 - \frac{1}{2}\sigma_{\beta_2}^2\beta_{20}^2k^4 \\ 0 \\ 2g_{12}\gamma_{10}P_0P_1\hat{R} \\ 2g_{12}\gamma_{20}P_0P_1\hat{R} \\ -\frac{1}{2}\beta_{20}k^2 + 2\gamma_{20}P_1^2\hat{R} \\ -\frac{1}{2}\beta_{10}k^2 + 2\gamma_{10}P_0^2\hat{R} \end{pmatrix}, \quad M_6 = \begin{pmatrix} 0 \\ 0 \\ 0 \\ 0 \\ 0 \\ -\frac{1}{2}\sigma_{\beta_1}^2\beta_{10}^2k^4 - \frac{1}{2}\sigma_{\beta_2}^2\beta_{20}^2k^4 \\ 0 \\ 0 \\ \frac{1}{2}\beta_{10}k^2 \\ \frac{1}{2}\beta_{20}k^2 \end{pmatrix},$$

$$M_7 = \begin{pmatrix} \beta_{10}k^2 \\ 0 \\ -\beta_{10}k^2 + 2\gamma_{10}P_0^2\hat{R} \\ 0 \\ 0 \\ 2g_{12}\gamma_{20}P_0P_1\hat{R} \\ -\sigma_{\beta_1}^2\beta_{10}^2k^4 \\ 0 \\ 0 \\ 0 \end{pmatrix}, \quad M_8 = \begin{pmatrix} 0 \\ \beta_{20}k^2 \\ 0 \\ -\beta_{20}k^2 + 2\gamma_{20}P_1^2\hat{R} \\ 0 \\ 2g_{12}\gamma_{10}P_0P_1\hat{R} \\ 0 \\ -\sigma_{\beta_2}^2\beta_{20}^2k^4 \\ 0 \\ 0 \end{pmatrix},$$

$$M_9 = \begin{pmatrix} 0 \\ 0 \\ 0 \\ 2g_{12}\gamma_{20}P_0P_1\hat{R} \\ -\frac{1}{2}\beta_{20}k^2 \\ -\frac{1}{2}\beta_{10}k^2 + 2\gamma_{10}P_0^2\hat{R} \\ 0 \\ 0 \\ -\frac{1}{4}\sigma_{\beta_1}^2\beta_{10}^2k^4 - \frac{1}{4}\sigma_{\beta_2}^2\beta_{20}^2k^4 \\ 0 \end{pmatrix}, \quad M_{10} = \begin{pmatrix} 0 \\ 0 \\ 2g_{12}\gamma_{10}P_0P_1\hat{R} \\ 0 \\ -\frac{1}{2}\beta_{10}k^2 \\ -\frac{1}{2}\beta_{20}k^2 + 2\gamma_{20}P_1^2\hat{R} \\ 0 \\ 0 \\ 0 \\ -\frac{1}{4}\sigma_{\beta_1}^2\beta_{10}^2k^4 - \frac{1}{4}\sigma_{\beta_2}^2\beta_{20}^2k^4 \end{pmatrix}.$$

References

1. G.P. Agrawal, *Nonlinear Fiber Optics*, 4th edition (Academic, 2008).
2. K. Tai, A. Hasegawa, A. Tomita, Phys. Rev. Lett. **56**, 135 (1986).
3. T.B. Benjamen, J.E. Feir, J. Fluid. Mech. **27**, 417 (1967).
4. A. Hasegawa, *Plasma Instabilities and nonlinear Effect* (Springer, Heidelberg, 1975).
5. L A. Ostrovskii, Sov. Phys. JETP **24**, 797 (1967).
6. Y.S. Kivshar, M. Peyrard, Phys. Rev. A **46**, 3198 (1992).

7. P.D. Miller, O. Band, Phys. Rev. E **57**, 6038 (1998).
8. Y.S. Kivshar, D. Anderson, M. Lisak, Phys. Scr. **47**, 679 (1993).
9. M. Soljacic *et al.*, Phys. Rev. Lett. **84**, 467 (2000).
10. J.F. Corney, O. Bang, Phys. Rev. Lett. **87**, 133901 (2001).
11. W. Krolikowski, O. Bang, J.J Rasmussen, J. Wyller, Phys. Rev. E **64**, 016612 (2001).
12. B.K. Esbensen, A. Wlotzka, M. Bache, O. Bang, W. Krolikowski, Phys. Rev. A **84**, 053854 (2011).
13. J. Wyller, W. Krolikowski, O. Bang, J.J. Rasmussen, Physica D **227**, 8 (2007).
14. N.I. Nikolov, O. Bang, J. Opt. Soc. Am. B **20**, 2329 (2003).
15. A. Dermican, U. Bandelow, Opt. Commun. **181**, 244 (2005).
16. J.R. Ott, M. Heuck, C. Agger, P.D. Rasmussen, O. Bang, Opt. Express. **16**, 25 (2008).
17. M.H. Frosz, A. stefani, O. Bang, Opt. Express **19**, 11 (2011).
18. B. Gu, W. Yuan, M.H. Frosz, A.P. Zhang, S. He, O. Bang, Opt. Lett. **37**, 5 (2012).
19. G.P. Agrawal, *Applications of Nonlinear Fiber Optics* (Academic Press, san Diego, 2001).
20. J.E. Rothenberg, Phys. Rev. Lett. **64**, 813 (1987).
21. P. Drummond, T. Kennedy, J. Dudley, Opt. Commun. **78**, 137 (1990).
22. Y. Kodama, A. Maruta, A. Hasegawa, Quantum Semiclass. Opt. **6**, 463 (1994).
23. G.P. Agrawal, Phys. Rev. Lett. **59**, 880 (1989).
24. F.Kh. Abdullaev, S.A. Darmanyan, S. Bischoff, M.P. Sorensen, J. Opt. Soc. Am. B **14**, 27 (1997).
25. M. Karisson, J. Opt. Soc. Am. B **15**, 2269 (1998).
26. A.G. Litvak *et al.*, Sov. J. Plasma Phys. **1**, 31 (1975).
27. H.L. Pecseli, J.J. Rasmussen, Plasma Phys. **22**, 421 (1980).
28. D. Suter, T. Blasberg, Phys. Rev. A **48**, 4583 (1993).
29. J.P. Gordon *et al.*, J. Appl. Phys. **36**, 3 (1965).
30. S. Akhmanov *et al.*, IEEE J. Quantum Electron. **4**, 568 (1968).
31. S. Gatz, J. Herrmann, Opt. Lett. **23**, 1176 (1998).
32. E.V. Doktorov, M.A. Molchan, Phys. Rev. A **75**, 053819 (2007).
33. E.V. Doktorov, M.A. Molchan, Phys. Scr. **76**, 558 (2007).
34. S.V. Manakov, Zh. Eksp. Teor. Fiz. **65**, 505 (1973) (Sov. Phys. JETP **38**, 248 (1974)).
35. R. Radhakrishnan, M. Lakshmanan, J. Phys. A **28**, 2683 (1995).
36. B. Prinari, M.J. Ablowitz, G. Biondini, J. Math. Phys. **47**, 063508 (2006).
37. R. Radhakrishnan, K. Aravinthan, Phys. Rev. E **75**, 066605 (2007).
38. M. Shen, H. Ding, Q. Kong, L. Ruan, S. Pang, J. Shi, Q. Wang, Phys. Rev. A **82**, 043815 (2010).
39. Z. Xu, Y.V. Kartashov, L. Torner, Phys. Rev. E **73**, 055601(R) (2006).
40. A. Alberucci, M. Peccianti, G. Assanto, A. Dyadyusha, M. Kaczmarek, Phys. Rev. Lett. **97**, 153903 (2006).
41. M. Shen, J.-J. Zheng, Q. Kong, Y.-Y. Lin, C.-C. Jeng, R.-K. Lee, W. Krolikowski, Phys. Rev. A **86**, 013827 (2012).
42. M. Shen, Q. Kong, C.-C. Jeng, L.-J. Ge, R.-K. Lee, W. Krolikowski, Phys. Rev. A **83**, 023825 (2011).
43. W. Chen, Q. Kong, M. Shen, Q. Wang, J. Shi, Phys. Rev. A **87**, 013809 (2013).
44. N. Ghofraniha, C. Conti, G. Ruocco, S. Trillo, Phys. Rev. Lett. **99**, 043903 (2007).
45. M. Peccianti, K. Brzdakiewicz, G. Assanto, Opt. Lett. **27**, 1460 (2002).
46. N.I. Nikolov, D. Neshev, O. Bang, W.Z. Krolikowski, Phys. Rev. E **68**, 036614 (2003).
47. P.V. Larsen, M.P. Sorensen, O. Bang, W.Z. Krolikowski, S. Trillo, Phys. Rev. E **73**, 036614 (2006).
48. M. Bache, O. Bang, J. Moses, F.W. Wise, Opt. Lett. **32**, 2490 (2007); M. Bache, O. Bang, W. Krolikowski, J. Moses, F.W. Wise, Opt. Express **16**, 3273 (2008).
49. J. Wyller, W.Z. Krolikowski, O. Bang, D.E. Peterson, J.J. Rasmussen, Phys. Rev. E **66**, 066615 (2002).
50. A.W. Snyder, D.J. Mitchell, Science **276**, 1538 (1997).
51. Q. Kong, Q. Wang, O. Bang, W. Krolikowski, Opt. Lett. **35**, 2152 (2010); Q. Kong, Q. Wang, O. Bang, W. Krolikowski, Phys. Rev. A **82**, 013826 (2010).
52. J. Garnier, F.Kh. Abdullaev, Physica D **145**, 65 (2000).
53. C.G.L. Tiofack, A. Mohamadou, T.C. Kofane, Opt. Commun. **283**, 1096 (2010).
54. A. Mohamadou, C.G.L. Tiofack, T.B. Ekogo, J. Atangana, T.C. Kofane, K. Porsezian, J. Mod. Opt. **58**, 924 (2011).
55. K. Furutsu, J. Res. Natl. Bur. Stand. Sect. D **67**, 303 (1963).
56. E.A. Novikov, Sov. Phys. JETP **20**, 1290 (1964).
57. W.H. Press, S.A. Teukolsky, W.T. Vetterling, B.P. Flannery, *Numerical Recipes in Fortran: The Art of Scientific Computing* (Cambridge University Press, Cambridge, 1992).